Numerical Study of Raceway Shape and Size in a Model Blast Furnace

Xing Peng, Jingsong Wang, Cong Li, Haibin Zuo, Xuefeng She, Guang Wang and Qingguo Xue

Abstract In ironmaking blast furnaces, hot air is injected through tuyeres to form a cavity, known as "raceway". In this study, a three-dimensional transient numerical model has been developed to study the shape and size of the raceway in a packed particle bed. It is assumed that gas and solid (particle) phases are interpenetrating continuum in the model. Gas phase turbulence is described as a k-ε dispersed model. Gas phase stress considers its effective viscosity. The solid phase constitutive relationship is expressed as solid stress that is characterized by solid pressure, bulk viscosity, kinetic viscosity, collisional viscosity, and frictional viscosity. The effects of blast velocity and injection angle on the raceway were studied. The results demonstrate when air is injected through the tuyere, the raceway size first increases, then decreases with time, and finally stabilizes. The raceway size increases with the increase of blast velocity. The raceway shape depends on the injection angle, and the surface area of the raceway is largest when the injection angle is 5°.

X. Peng · J. Wang (✉) · C. Li · H. Zuo · X. She · G. Wang · Q. Xue
State Key Laboratory of Advanced Metallurgy, University of Science and Technology Beijing, Beijing 100083, People's Republic of China
e-mail: wangjingsong@ustb.edu.cn

X. Peng
e-mail: pengxing_hunan@sina.com

C. Li
e-mail: licong2004@yeah.net

H. Zuo
e-mail: zuohaibin@ustb.edu.cn

X. She
e-mail: shexuefeng@ustb.edu.cn

G. Wang
e-mail: wangguang@ustb.edu.cn

Q. Xue
e-mail: xueqingguo@ustb.edu.cn

The Minerals, Metals & Materials Society (ed.), *TMS 2020 149th Annual Meeting & Exhibition Supplemental Proceedings*, The Minerals, Metals & Materials Series, https://doi.org/10.1007/978-3-030-36296-6_100

Keywords Raceway shape · Raceway size · Euler multiphase flow · Blast velocity · Injection angle

Introduction

The raceway is specified as a cavity zone formed in a particle packed or moving bed with particles' circulation due to intensive fluid–solid interactions. In ironmaking blast furnaces, the raceway is formed by injecting hot air through tuyeres. The combustion of coke and injected fuels in the raceway will supply gas and heat for the critical endothermic reduction of iron ores and the smelting of iron [1]. Therefore, the raceway shape and size will directly affect the primary distribution of the gas and heat inside the blast furnace. For the blast furnace to operate efficiently and stably for increasing iron production, it is necessary to understand the key factors influencing of the raceway shape and size.

The research on the blast furnace raceway shape and size can be divided into three methods: theoretical analysis, experimental test, and numerical simulation. In theoretical analysis, a few researchers analyze the size of the raceway based on the force balance of the raceway boundary [2–4]. However, this method treats the raceway as a circle or sphere and ignores the force between the particles, which is a relatively crude method. In terms of experimental testing, the complex environment of high temperature and pressure in the raceway has introduced significant difficulties to direct research. Thus, in the past, the raceway depth and boundary shape were mainly examined in cold models [5–7]; however, it was difficult to obtain dynamic information experimentally and to accurately measure the raceway shape and size in three-dimensional space. Therefore, to overcome these difficulties in theoretical and experimental studies, combined continuum and discrete modeling (CCDM) was developed [8–10]. CCDM is used to obtain microscopic information that aids the understanding of the flow characteristics. The effects of various conditions on the raceway shape and size were investigated. Nonetheless, CCDM studies generally used two-dimensional geometries and were computationally expensive. The Eulerian multiphase flow model (EMFM) based on the continuous method can be applied well to three-dimensional scale, high efficiency, and low computational cost. The shape and size of the raceway are studied with a two-dimensional condition using transient [11] or steady [12] model base on continuous method. Rangarajan et al. [13] extensively studied the influence of the operating conditions and physical parameters on raceway properties using a two-fluid model. However, no details on constitutive relations can be found in the article.

In this study, a three-dimensional transient numerical model based on the continuous method was developed. This model uses more comprehensive constitutive relations to describe the stress term of the momentum equation. The effect of blast velocity and blast injection angle on raceway shape and size are investigated in a model blast furnace.

Model Description

From the perspective of the blast furnace ironmaking process, the influence of the thermochemical reaction in the raceway is reflected in the change of gas flow. Therefore, the isothermal solution of the velocity field is sufficient to predict the raceway shape and size. For simplicity, this study did not consider reaction or heat transfer. It is assumed that the isothermal flow conditions predict the shape of the raceway without burning. The different phases are present in the same computational volume simultaneously and are characterized by the volume fraction, α_i, of each phase i (gas, solid). The conservation equations of mass and momentum are solved for each phase in a Eulerian frame. The role of the constitutive equation is to describe the essential characteristics of the gas and solid phases and to close the conservation equation.

Conservation Equations

In the process of gas–solid flow, gas and particle flow satisfy the conservation of mass and momentum. Because there is no mass exchange between solid particles and gas phase, they are independent of each other. The mass conservation equation for phase i can be expressed as

$$\frac{\partial(\alpha_i \rho_i)}{\partial t} + \nabla \cdot (\alpha_i \rho_i U_i) = 0, \tag{1}$$

$$\Sigma \alpha_i = 1 \tag{2}$$

where ρ_i is the density and U_i is the velocity vector of phase i.

The interaction force between gas and particle is very complex. It includes drag, lift, additional mass, and basset force, etc. However, in general, not all forces need be considered. In the blast furnace condition, the particle diameter is larger, and the density of the gas is much smaller than the density of the particles. Therefore, the drag force between phases is generally considered in the gas–solid flow process. The momentum conservation equation for phase i can be written as

$$\frac{\partial(\alpha_i \rho_i U_i)}{\partial t} + \nabla \cdot (\alpha_i \rho_i U_i U_i) = \nabla \cdot \tau_i + \alpha_i \rho_i g + S \tag{3}$$

where τ_i is the stress tensor, and g is gravity acceleration. The source term, S, is generated by momentum transfer between the gas and solid phases and is expressed as

$$S = \beta\big(U_j - U_i\big), \quad j \neq i \tag{4}$$

where β is the momentum exchange coefficient. For $\alpha_g > 0.8$, the coefficient β is based on the drag force of the fluid acting on a single particle, and for $\alpha_g \leq 0.8$, the coefficient is described by Ergun's equation [14]. β can be expressed as

$$\beta = \begin{cases} \frac{3}{4} C_D \frac{\alpha_s \alpha_g \rho_g |U_s - U_g|}{d_s} \alpha_g^{-2.65} & \alpha_g > 0.8 \\ 150 \frac{\alpha_s^2 \mu_g}{\alpha_g d_s^2} + 1.75 \frac{p_g \alpha_s |U_s - U_g|}{d_s} & \alpha_g \leq 0.8 \end{cases} \tag{5}$$

where d_s is solid (particle) diameter, and the drag coefficient, C_D, is given by

$$C_D = \begin{cases} \frac{24}{\alpha_g \mathrm{Re}} \left[1 + 0.15 (\alpha_g \mathrm{Re})^{0.687} \right] & \mathrm{Re} \leq 1000 \\ 0.44 & \mathrm{Re} > 1000 \end{cases} \tag{6}$$

Re is the particle Reynolds number and can be expressed as

$$\mathrm{Re} = \frac{\rho_g d_s |U_s - U_g|}{\mu_g} \tag{7}$$

Constitutive Relations

The gas phase constitutive equation is featured by gas effective viscosity. The solid phase constitutive relationship is expressed as the solid stress, which is characterized by the solid pressure, bulk viscosity, kinetic viscosity, collisional viscosity, and frictional viscosity. A detailed description of the constitutive relations is summarized in Table 1 [14–18].

Turbulence Equations

Turbulent predictions are obtained from the k-ε dispersed model. The transport equations are:

$$\frac{\partial}{\partial t} (\alpha_g \rho_g k_g) + \nabla \cdot (\alpha_g \rho_g U_g k_g) = \nabla \cdot \left(\alpha_g \frac{\mu_{t,g}}{\sigma_k} \nabla k_g \right) + \alpha_g G_{k,g} - \alpha_g \rho_g \varepsilon_g + \alpha_g \rho_g \Pi_{k_g} \tag{8}$$

$$\frac{\partial}{\partial t} (\alpha_g \rho_g \varepsilon_g) + \nabla \cdot (\alpha_g \rho_g U_g \varepsilon_g) = \nabla \cdot \left(\alpha_g \frac{\mu_{t,g}}{\sigma_\varepsilon} \nabla \varepsilon_g \right) + \alpha_g \frac{\varepsilon_g}{k_g} (C_{1\varepsilon} G_{k,g} - C_{2\varepsilon} \rho_g \varepsilon_g) + \alpha_g \rho_g \Pi_{\varepsilon_g} \tag{9}$$

Table 1 Constitutive relations

Gas stress: $\tau_g = -P_g I + \mu_{\text{eff},g}(\nabla U_g + (\nabla U_g)^T) - \frac{2}{3}(\mu_{\text{eff},g}(\nabla \cdot U_g)I + \rho_g k_g)$
Gas effective viscosity: $\mu_{\text{eff},g} = \mu_g + \mu_{t,g}$
Gas turbulent viscosity: $\mu_{t,g} = \rho_g C_\mu \frac{k_g^2}{\varepsilon_g}$
Solid stress: $\tau_s = (-P_s + \xi_s \nabla \cdot U_s)I + \mu_s\{(\nabla U_s + \nabla U_s^T) - \frac{2}{3}\nabla U_s I\}$
Solid pressure: $P_s = \alpha_s \rho_s \Theta + 2\rho_s(1+e)\alpha_s^2 g_0 \Theta$
Particle transport equation: $\frac{3}{2}\left[\frac{\partial(\rho\alpha\Theta)}{\partial t} + \nabla \cdot (\rho_s \alpha_s U_s \Theta)\right] = \tau_s : \nabla U_s + \nabla \cdot (k_s \nabla \Theta) - \gamma_s - 3\beta\Theta$
Diffusion coefficient: $k_s = \frac{150\rho_s d_s \sqrt{\Theta\pi}}{384(1+e)g_0}\left[1 + \frac{6}{5}g_0\alpha_s(1+e)\right]^2 + 2\alpha_s^2\rho_s d_s g_0(1+e)\left(\frac{\Theta}{\pi}\right)^{1/2}$
Particle collisional dissipation of energy: $\gamma_s = 3(1-e^2)g_0\rho_s\alpha_s^2\Theta\left(\frac{4}{d_s}\left(\frac{\Theta}{\pi}\right)^{1/2} - \nabla \cdot U_s\right)$
Solid radial distribution function: $g_0 = \frac{3}{5}\left[1 - \left[\frac{\alpha_s}{\alpha_{s,\max}}\right]^{1/3}\right]^{-1}$
Solid bulk viscosity: $\xi_s = \frac{4}{3}\alpha_s^2\rho_s d_s g_0(1+e)\left(\frac{\Theta}{\pi}\right)^{1/2}$
Solids shear stresses: $\mu_s = \mu_{s,\text{col}} + \mu_{s,\text{kin}} + \mu_{s,\text{fr}}$
Solid kinetic viscosity: $\mu_{s,\text{kin}} = \frac{10\rho_s d_s\sqrt{\Theta\pi}}{96(1+e)g_0}\left[1 + \frac{4}{5}g_0\alpha_s(1+e)\right]^2$
Solid collisional viscosity: $\mu_{s,\text{col}} = \frac{4}{5}\alpha_s^2\rho_s d_s g_0(1+e)\left(\frac{\Theta}{\pi}\right)^{1/2}$
Solid frictional viscosity: $\mu_{s,\text{fr}} = \frac{P_{\text{friction}}\sin\phi}{2\sqrt{I_{2D}}}$
Frictional pressure: $P_{\text{friction}} = \begin{cases} \text{Fr}\frac{(\alpha_s - \alpha_{s,\min})^n}{(\alpha_{s,\max} - \alpha_s)^p}, & \text{Fr} = 0.1\alpha_s,\ n = 2,\ p = 5 \quad \alpha_s \geq 0.5 \\ 0 & \alpha_s < 0.5 \end{cases}$

Here, $G_{k,g}$ is the production of turbulent kinetic energy in the gas phase. Π_{k_g} and Π_{ε_g} are source terms that can be included to model the influence of the dispersed phases on the continuous phase.

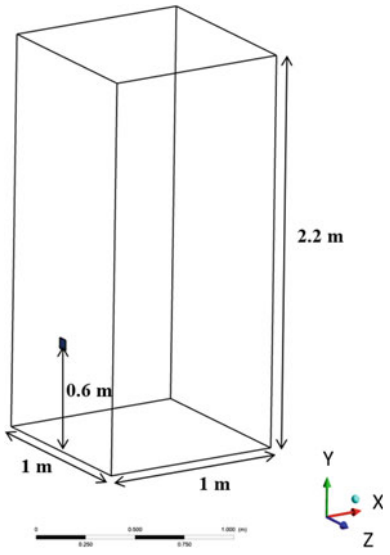

Fig. 1 Geometric model

Table 2 Simulation parameters

Parameters	Value
Number of calculation units	64,960
Time step	0.0001 s
Blast injection angle	0°, 5°, 10°
Blast velocity	150, 175, 200, 225, 250, 275, 300 m/s
Particle density	1000 kg/m^3
Particle diameter	10 mm
Angle of internal friction	30°
Initial porosity of the bed	0.6
Initial bed height	2 m

Geometry and Operating Conditions

The EMFM equations were calculated based on the framework of software package ANSYS Fluent. The maximum residual at convergence is set to 1×10^{-3} for combined continuity and momentum equations, turbulent kinetic energy, and turbulent dissipation equations. As shown in Fig. 1, the computing domain is a cuboid with length of 1 m, width of 1 m, and height of 2.2 m. The tuyere is a square with $D_t = 0.056$ m, the height of the tuyere is $H_t = 0.6$ m, and the center of the tuyere is 0.5 m from the side wall. Air is injected into the packed bed from the tuyere. The injection angle of 5° and 10° is inclined to the negative direction of the y-axis. The simulation parameters are listed in Table 2. The number of calculation units used for

the numerical experiments was 64,960, showing that further refinement of the grid in either direction did not change the result by more than 2.5%.

Results and Discussion

In this study, when the solid volume fraction is less than 0.5, the friction pressure is 0, and the solid motion is mainly affected by collision. Therefore, the boundary of the raceway is defined as solid volume fraction of 0.5. A typical blast velocity can be close to 250 m/s in the tuyere of a small blast furnace. Figure 2 shows time evolution of the solid volume fraction for a blast velocity of 250 m/s in injection angle 5°. When air is injected through the tuyere, the size of the raceway first increases, then decreases with time, and then stabilizes at 5 s. This is because when the solid phase interacts with the gas phase, the initial solid phase volume fraction changes toward the maximum limiting volume fraction and eventually stabilizes, controlled by the momentum conservation equation.

Raceway Shape Characteristics

Figure 3 shows the solid volume fraction for a blast velocity 250 m/s. The depth and height of the raceway change significantly at different injection angles. The three-dimensional shape of the raceway is shown in Fig. 4. The shape of the raceway is

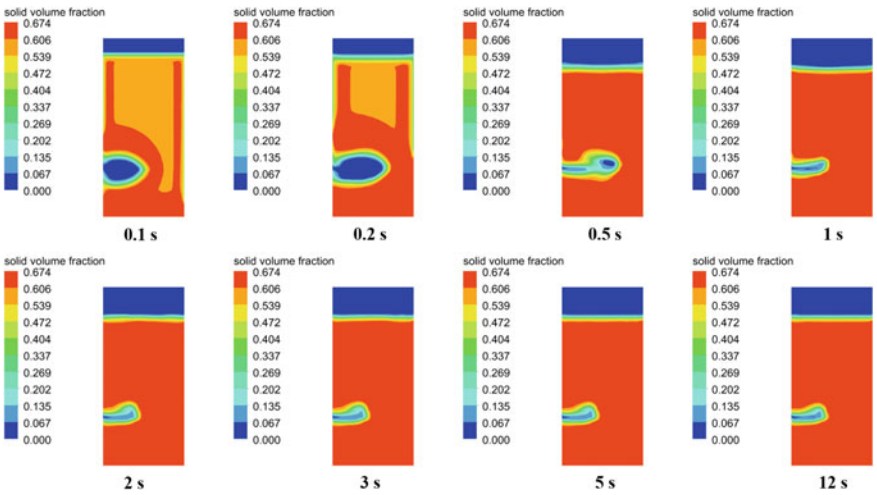

Fig. 2 Time evolution of solid volume fraction for blast velocity 250 m/s with an injection angle of 5° (plane $Z = 0.5$ m)

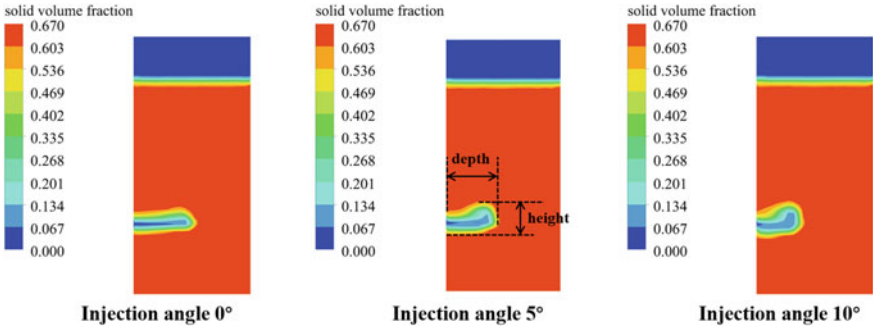

Fig. 3 Solid volume fraction for blast velocity 250 m/s (plane $Z = 0.5$ m)

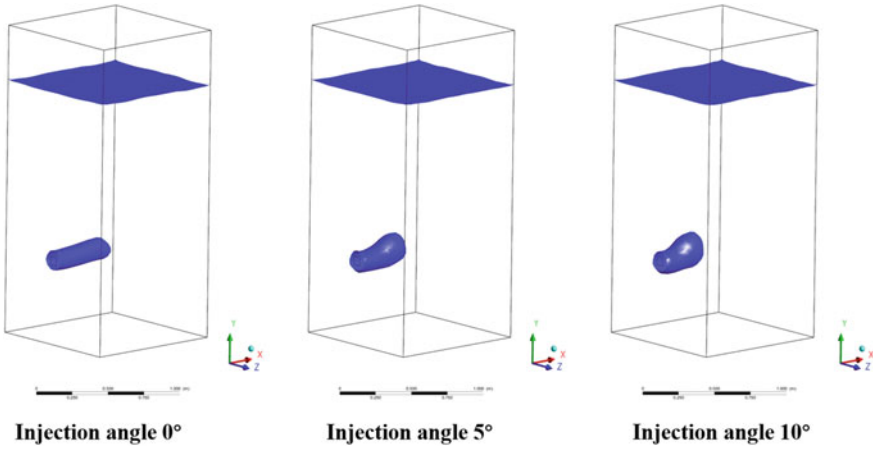

Fig. 4 Effect of injection angle on raceway shape and size for blast velocity 250 m/s

characterized by an upturned sac that is consistent with the results obtained from actual blast furnace anatomy.

In order to analyze the shape of the raceway, the ratio of height to depth of the raceway is taken as Φ. As shown in Fig. 5, when the injection angle is 0° and 5°, Φ decreases first and then increases with an increase in the blast velocity. This is because in that velocity range, the depth of the raceway is affected more than the height. Furthermore, the effect of the blast velocity on Φ is only slight with an injection angle 0°. However, when the injection angle is 10°, Φ increases with an increase in the blast velocity, indicating that under this condition, the blast velocity has a more significant influence on the height of the raceway. Φ increases as the injection angle increases, and the effect of the injection angle is greater than that of blast velocity. Therefore, the raceway shape depends on the injection angle.

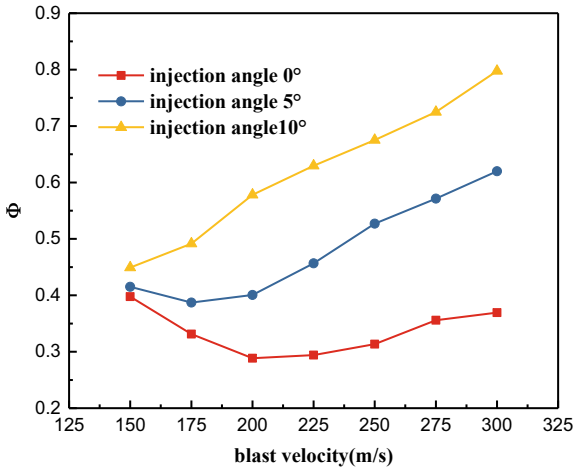

Fig. 5 Effect of blast velocity and injection angle on Φ

Raceway Size Characteristics

Figure 6 shows the effect of blast velocity and injection angle on the depth and height of the raceway. The increase in the blast velocity is beneficial to increase the depth and height of the raceway. However, the increase in the injection angle increases the height of the raceway as shown in Fig. 6b, but the depth of the raceway decreases as shown in Fig. 6a. This is attributed to the fact that the velocity component in the negative direction of the y-axis increases the drag force in the vertical direction, while the velocity in the positive direction of the x-axis relative decreases, and the drag force decreases.

Figure 7 shows that the surface area of the raceway increases significantly as the blast velocity increases. However, the effect of the injection angle is not significant. It

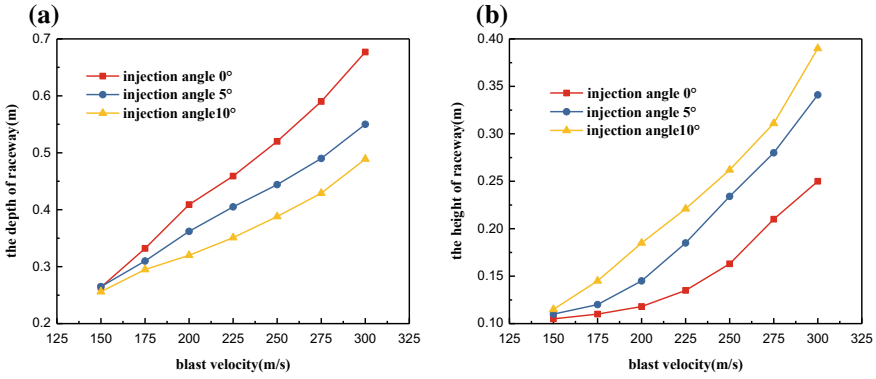

Fig. 6 Effect of blast velocity and injection angle on the depth and height of raceway

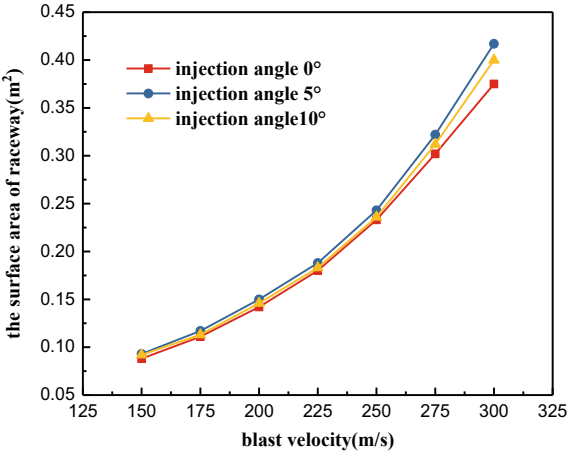

Fig. 7 Effect of blast velocity and injection angle on the surface area of the raceway

is interesting that the surface area of the raceway is largest when the injection angle is 5°. The reason is that when the injection angle exceeds a certain angle, the gas–solid momentum is exchanged along the y-axis direction, while exchange is reduced along the x-axis direction; however, the velocity along the y-axis direction is reduced more rapidly due to gravity in the solid phase in the vertical direction. Compared with the influence of the blast velocity, the change in the injection angle has little effect on the surface area of the raceway; however, selecting the appropriate injection angle can increase the surface area of the raceway in with the same blast kinetic energy, which is beneficial to the particle collision movement in the raceway and reasonable distribution of gas flow in the lower part of the blast furnace.

Conclusion

A three-dimensional transient numerical model has been developed to study the shape and size of the raceway in the packed particle bed of a model blast furnace. The comprehensive constitutive relation of gas phase and solid phase is considered in the model. The major conclusions from the study are as follows:

(1) When air is injected through the tuyere, the raceway size first increases, then decreases with time, and finally stabilizes.
(2) The size (surface area, depth, and height) of the raceway increases with an increase in blast velocity.
(3) The increase in the injection angle increases the height of the raceway, but the depth decreases.
(4) The raceway shape depends on the injection angle, and the surface area of the raceway is largest when the injection angle is 5°.

Acknowledgements The authors gratefully acknowledge the financial support of the National Natural Science Foundation of China (No. U1960205) and State Key Laboratory of Advanced Metallurgy (No. 41618029).

References

1. Burgess JM (1985) Fuel combustion in the blast furnace raceway zone. Prog Energy Combust Sci 11(1):61–82
2. Gupta GS, Rajneesh S, Singh V, Sarkar S, Rudolph V, Litster JD (2005) Mechanics of raceway hysteresis in a packed bed. Metall Mater Trans B 36(6):755–764
3. Guo J, Cheng S, Zhao H, Pan H, Du P, Teng Z (2013) A mechanism model for raceway formation and variation in a blast furnace. Metall Mater Trans B 44(3):487–494
4. Li YL, Cheng SS, Zhang P, Guo J (2016) Development of 3-D mathematical model of raceway size in blast furnace. Ironmak Steelmak 43(4):308–315
5. Sastry GSSRK, Gupta GS, Lahiri AK (2003) Cold model study of raceway under mixed particle conditions. Ironmak Steelmak 30(1):61–65
6. Rajneesh S, Sarkar S (2004) Prediction of raceway size in blast furnace from two dimensional experimental correlations. ISIJ Int 44(8):1298–1307
7. Mojamdar V, Gupta GS, Puthukkudi A (2018) Raceway formation in a moving bed. ISIJ Int 58(8):1396–1401
8. Umekage T, Yuu S, Kadowaki M (2005) Numerical simulation of blast furnace raceway depth and height, and effect of wall cohesive matter on gas and coke particle flows. ISIJ Int 45(10):1416–1425
9. Singh V, Gupta GS, Sarkar S (2007) Study of gas cavity size hysteresis in a packed bed using DEM. Chem Eng Sci 62(22):6102–6111
10. Miao Z, Zhou Z, Yu AB, Shen Y (2017) CFD-DEM simulation of raceway formation in an ironmaking blast furnace. Powder Technol 314:542–549
11. Mondal SS, Som SK, Dash SK (2005) Numerical predictions on the influences of the air blast velocity, initial bed porosity and bed height on the shape and size of raceway zone in a blast furnace. J Phys D Appl Phys 38(8):1301
12. Sarkar S, Gupta GS, Kitamura SY (2007) Prediction of raceway shape and size. ISIJ Int 47(12):1738–1744
13. Rangarajan D, Shiozawa T, Shen Y, Curtis JS, Yu A (2013) Influence of operating parameters on raceway properties in a model blast furnace using a two-fluid model. Ind Eng Chem Res 53(13):4983–4990
14. Gidaspow D. (1994). Multiphase flow and fluidization: continuum and kinetic theory descriptions. Academic Press
15. Ding J, Gidaspow D (1990) A bubbling fluidization model using kinetic theory of granular flow. AIChE J 36(4):523–538
16. Lun CKK, Savage SB, Jeffrey DJ, Chepurniy N (1984) Kinetic theories for granular flow: inelastic particles in couette flow and slightly inelastic particles in a general flowfield. J Fluid Mech 140:223–256
17. Schaeffer DG (1987) Instability in the evolution equations describing incompressible granular flow. J Differ Equat 66(1):19–50
18. Ocone R, Sundaresan S, Jackson R (1993) Gas-particle flow in a duct of arbitrary inclination with particle-particle interactions. AIChE J 39(8):1261–1271